Coupling of supra-to sub-salt structures during gravity gliding : A physical analogue modelling investigation

Sian L. Evans, Christopher A-L. Jackson, Sylvie Schueller, Jean-Marie Mengus

Journal of Structural Geology 185 (2024) 105171

Contents lists available at ScienceDirect

Journal of Structural Geology

journal homepage: www.elsevier.com/locate/jsg

Coupling of supra-to sub-salt structures during gravity gliding: A physical analogue modelling investigation

Sian L. Evans [a,*,1], Christopher A-L. Jackson [a,2], Sylvie Schueller [b], Jean-Marie Mengus [b]

[a] Basins Research Group, Department of Earth Science and Engineering, Imperial College London, London, UK
[b] IFP Energies Nouvelles, Rueil-Malmaison, France

A B S T R A C T

Viscous salt layers can introduce significant structural complexity to the basins in which they are deposited. Along basin margins, salt typically flows basinward due to regional tilting of the margin, and can be influenced by the geometry of the surface that it flows over (e.g. fault scarps on the base-salt surface). This interaction can lead to coupling of sub- and supra-salt structures, with the orientation and distribution of base-salt structures reflected in the structure of the overburden. However, the controls on the degree of strain coupling during salt-detached translation are relatively poorly understood, in particular the roles played by the thickness and mechanical heterogeneity of the salt unit. This is, in part, caused by difficultly in deconvolving the relative contribution of variables such as salt thickness, the magnitude of base-salt relief, sediment supply, and regional tectonic regime. In addition, seismic reflection data provide only the present structure of the basin, from which its evolution must be inferred.

To evaluate the influence of salt thickness and heterogeneity on sub-to supra-salt strain coupling during salt-detached translation in the extensional domain, we present a series of physical analogue models with controlled boundary conditions. We use a model apparatus with a simple geometry comprising three oblique basal steps, and vary the thickness and composition of the salt analogue in each experiment to evaluate the proposed variables. X-ray tomography allows us to image the internal structure during model evolution and therefore gain a 4D view of its structural development. Results show that supra-salt structures associated with thicker and more homogeneous salt units are characterised by symmetric extensional structures and large diapirs, with significant vertical and lateral displacements and only weak coupling to the underlying base-salt relief. Conversely, thinner and more heterogeneous salt units are characterised by asymmetric extensional structures and primary welds, with restricted vertical displacement, such that the resultant overburden structure is strongly coupled to the geometry of the base-salt surface. These results document the important role of base-salt relief in the structural evolution of salt basins and provide model analogues that are valuable assets in seismic interpretation efforts on salt-influenced basin margins.

1. Introduction

By deforming in a viscous manner over geological timescales, mobile salt layers introduce unique structural complexity to the basins in which they are deposited. Salt tectonics on passive margins is primarily gravity-driven, with two dominant driving mechanisms: gravity gliding, where gravitational instability is induced by tilting of the margin, and gravity spreading, where gravitational instability is induced by differential loading (e.g. Schultz-Ela, 2001; Rowan et al., 2004; Brun and Fort, 2011; Rowan et al., 2012; Peel, 2014). These models represent end-members of a spectrum, and typically both gliding and spreading act contemporaneously to drive salt flow and supra-salt deformation, though their relative contributions may vary (Schultz-Ela, 2001; Rowan et al., 2012; Peel, 2014; Allen et al., 2016). For example, the Angolan margin is interpreted to be dominated by gravity gliding, whereas the present Gulf of Mexico is interpreted to be dominated by gravity spreading (Schultz-Ela, 2001). Natural salt basins can sit anywhere on this spectrum, depending on the geological setting, which to a large extent controls their structural development.

However, classic models of gliding and spreading tend to envisage a perfectly smooth base of salt, gently dipping towards the centre of the basin (e.g. Brun and Fort, 2011). Such smooth surfaces are rare in nature, and while the simplified models broadly explain the development of large-scale, kinematically-linked domains of extension and contraction, they do not adequately account for the wide variety of structural styles observed on many passive margins (e.g. Dooley et al., 2017; Pichel et al., 2019b; Evans and Jackson, 2020; do Amarante et al., 2021). One reason for this is that the base-salt surface is often rugose due to either pre-salt or syn-salt tectonic events, creating residual topography upon which the evaporites are deposited, or post-salt tectonic events that

* Corresponding author.
E-mail address: sian.lianne@outlook.com (S.L. Evans).
[1] Present address: Department of Geosciences, University of Oslo, Oslo, Norway.
[2] Present address: Jacobs, Manchester, UK.

https://doi.org/10.1016/j.jsg.2024.105171
Received 14 November 2023; Received in revised form 22 May 2024; Accepted 22 May 2024
Available online 23 May 2024

reactivate or create new thick-skinned structures. For example, in the former case, when salt is deposited shortly after rifting, the residual topography is defined by relief associated with syn-rift normal fault scarps (e.g. offshore Angola; Fig. 1). As the salt accumulates, it buries this pre-existing relief, thinning over topographic highs and thickening into topographic lows. When gravitational instability is then induced due to tilting of the basin, the mobile salt flows basinward over the rugose basal surface.

Several previous seismic-based studies have inferred how the structural development of salt basins may be influenced by relief on the base-salt surface during gravitationally-driven, salt-detached translation. For example, in the translational domain of the Kwanza Basin, offshore Angola, studies have suggested that the development of supra-salt structures was influenced by salt flow over fault scarps at the base-salt, resulting in great structural complexity (e.g. Rowan et al., 2004; Jackson and Hudec, 2005; Evans and Jackson, 2020; Erdi and Jackson, 2021). Similarly, offshore Brazil, salt flux variations caused by translation across large base-salt highs are interpreted to have resulted in simultaneous development of extensional and contractional supra-salt structures (Dooley et al., 2017; Pichel et al., 2020; do Amarante et al., 2021). A similar process has also been proposed offshore Morocco, where the pre-salt topography is inferred to have controlled depositional salt thickness and the distribution of supra-salt structures during gravity-driven translation (Pichel et al., 2019b). Finally, in the Mediterranean, local rates of salt flow and supra-salt deformation are suggested to be modulated by large base-salt anticlines in the Levant Basin (Evans et al., 2021), and by sub-salt seamounts in the Liguro-Provençal Basin (Ferrer et al., 2017).

Physical and numerical modelling studies have supported these interpretations of natural systems. Physical analogue models investigating the impact of base-salt relief have demonstrated that lateral salt flow over a step in the base of salt creates volumetric imbalances in the flow of salt (e.g. Gaullier et al., 1993; Dooley et al., 2017; Dooley and Hudec, 2017; Roma et al., 2018; Dooley et al., 2020). This process facilitates 'coupling' of the sub- and supra-salt structures, even where the base-salt structures have been inactive since salt deposition (e.g. Gaullier et al., 1993; Dooley et al., 2017; Roma et al., 2018). Numerical models have similarly supported the importance of pre-salt structural inheritance and shown that variables such as base-salt dip, step height and connectivity between salt sub-basins are important controls on the interaction of sub- and supra-salt structures (e.g. Gradmann and Beaumont, 2017; Pichel et al., 2019a).

Advancing the important findings of these previous studies, this study constrains the influence of additional variables such as salt thickness and heterogeneity on supra-salt deformation over non-planar base-salt relief during gravity-driven translation in the updip extensional domain. Several studies suggested that the apparent strong influence of sub-salt structures on supra-salt structures in the Kwanza Basin, offshore Angola, was due to the magnitude of relief relative to the thickness of the salt layer (Rowan et al., 2004; Jackson and Hudec, 2005; Evans et al., 2020). Furthermore, many salt layers are not composed purely of halite, but are interbedded with carbonates, siliciclastics or other evaporites such as anhydrite (e.g. Cartwright et al., 2012; Jackson et al., 2015; Rowan et al., 2019). These composite salt layers, known as

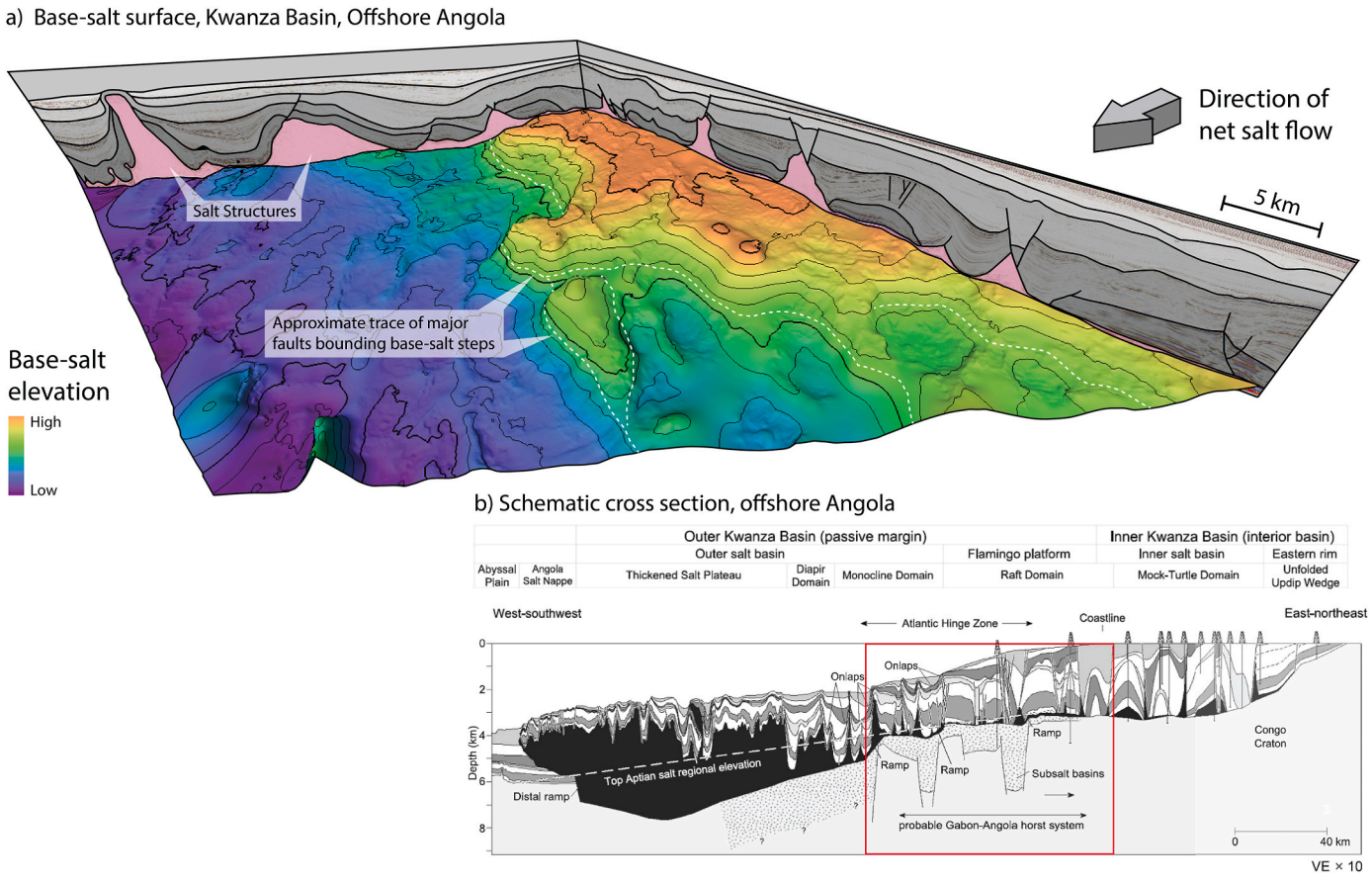

Fig. 1. a) Base-salt surface in the Kwanza Basin, offshore Angola, mapped from 3D seismic volume. Surface shows residual topographic relief due to fault scarps inherited from earlier rifting. Interpreted seismic sections show supra-salt structures and associated traps. See Evans and Jackson (2020) for more information. b) Schematic regional cross section of the Angolan margin from shelf to distal salt nappe. Several large ramps are shown to offset the base-salt. Red box indicates approximate area analogous to models presented in this study. Modified from Hudec and Jackson (2004). (For interpretation of the references to colour in this figure legend, the reader is referred to the Web version of this article.)

layered evaporite sequences, are rheologically stratified, containing both strong and weak layers that determine how the salt layer accommodates strain during gravity-driven deformation (Cartwright et al., 2012; Rowan et al., 2019). By controlling the deformation of the salt layer itself, the intra-salt heterogeneity implicitly affects the structural development of the overburden. In this study, we seek to understand how both the thickness of the salt and its mechanical stratification can affect the relationship between sub- and supra-salt structures.

By using a physical modelling approach we are able to shed new light on the influence of these variables on overburden deformation, and how they control the relationship between supra-salt structures and underlying base-salt relief. Seismic reflection data reveal only the present-day structure, whereas models (physical or numerical) allow us to observe how, when and where supra-salt structures evolve. Physical models test these concepts by creating a 3D, scaled-down approximation of a natural system, colloquially referred to as a 'sandbox model'. Such models allow observation of salt structure development on a human timescale (i.e. minutes to weeks, rather than millions of years), and have played a vital role in achieving our present understanding of salt-tectonic systems (e.g. Vendeville and Cobbold, 1988; Vendeville, 1988, 1989; Cobbold et al., 1989; Richard, 1991; Vendeville and Jackson 1992a,b). Most importantly, they allow us to isolate the influence of specific variables (e.g. salt rheology, thickness, strain rate) under precisely controlled boundary conditions. This method therefore gives us an opportunity to test and further develop the interpretations made in seismic reflection-based studies of natural systems.

We use physical models to investigate how the depositional thickness of the salt layer and its rheology control the coupling of supra-salt structures to steps on the base-salt. We use CT (Computer Tomography) scanning which images the models in 3D, enabling us to observe the internal deformation of the models as they evolve. By varying the thickness and composition of the salt analogue in controlled, gravity-driven experiments, we investigate how these variables influence the coupling between sub- and supra-salt structures. Herein we use the term 'coupled' in the spatial sense, where sub-salt structures influence the genesis of supra-salt structures (as opposed to the geometric sense, which implies sub- and supra-salt structures are hard-linked e.g. Vendeville and Jackson, 1992a; Stewart et al., 1997; Withjack and Callaway, 2000). We therefore define a 'strongly coupled' system as one in which the location and orientation of supra-salt structures are clearly controlled by the underlying sub-salt structures. A 'weakly coupled' system is defined one in which a relationship is observed but less apparent, whereas in a 'decoupled' system there is no apparent influence of sub-salt structures on supra-salt structural style.

2. Model set-up

2.1. Base of model design

To investigate the extent and style of supra-to sub-salt coupling during salt-detached translation, we designed a model base with a simple, downward-stepping geometry (Fig. 2). The model steps were designed to reflect natural base-salt geometries observed offshore Angola (Fig. 1) and other salt basins around the world in a simplified form. This set-up allows us to explicitly model the influence of the basal steps on the overburden structure. It is important to note that the goal of the physical modelling study is not to directly reproduce specific structures observed offshore Angola, but to create a simplified scenario based on the natural system that allows us to isolate the effects of the chosen variables.

The base of the model, representing the base-salt surface, comprises three downdip-facing steps striking parallel and sub-parallel to the model boundary (Fig. 2). We chose three distinct orientations to make it easier to directly correlate the coupling of supra-salt structures to the underlying base-salt steps, thus reducing ambiguity in the model results. The basal steps are 1 cm high, equivalent to approximately 1 km when scaled (see Section 2.2), which is comparable to the height of fault scarps observed at the base-salt offshore Angola (Evans and Jackson, 2020). The model steps are built out of plasticard and covered with a rhodoïd foil. The basin-facing planes dip at an angle comparable to typical rift-related normal faults (60°), with the corner of each step slightly rounded to evoke minor footwall erosion.

The downward-stepping basal geometry and direction of flow induced by tilting was the same for each experiment. We varied only the thickness and heterogeneity of the salt analogue in the initial set-up of each experiment to isolate the effects of these variables (Fig. 3; Table 2).

2.2. Scaling

In order to replicate geological processes on human time and length scales, physical properties of the natural system must be scaled appropriately (Hubbert, 1937; Ramberg, 1981). The rheological behaviour of the analogue materials must mimic processes that naturally occur over millions of years and over tens of kilometres. The scaling consists of considering the length scale ratio (geometric ratio), the time scale ratio (kinematic ratio) and the viscosity ratio (derived from the dynamic ratio) since gravity, cohesion and densities are in the same order of magnitudes between the model and the reality. By selecting the length and viscosity ratios, the time scale ratio is also fixed (such that viscosity ratio = length ratio x time ratio). The scaling relationships used in our models are presented in Table 1 and described below.

The models presented herein focus on modelling salt flow over base-salt steps in the proximal, extension-dominated domain of a salt-detached slope, and the inboard part of the translational domain, at a

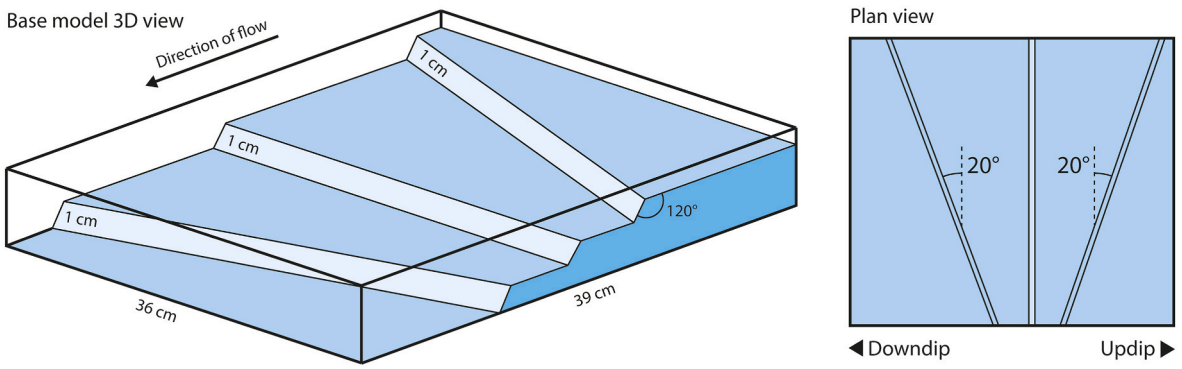

Fig. 2. Basal geometry of physical analogue models designed to investigate the development of supra-salt structures during gravity-driven extension and translation. The model consists of three basin-facing steps oriented at different angles. Steps represent inherited topography of syn-rift fault scarps on passive margins.

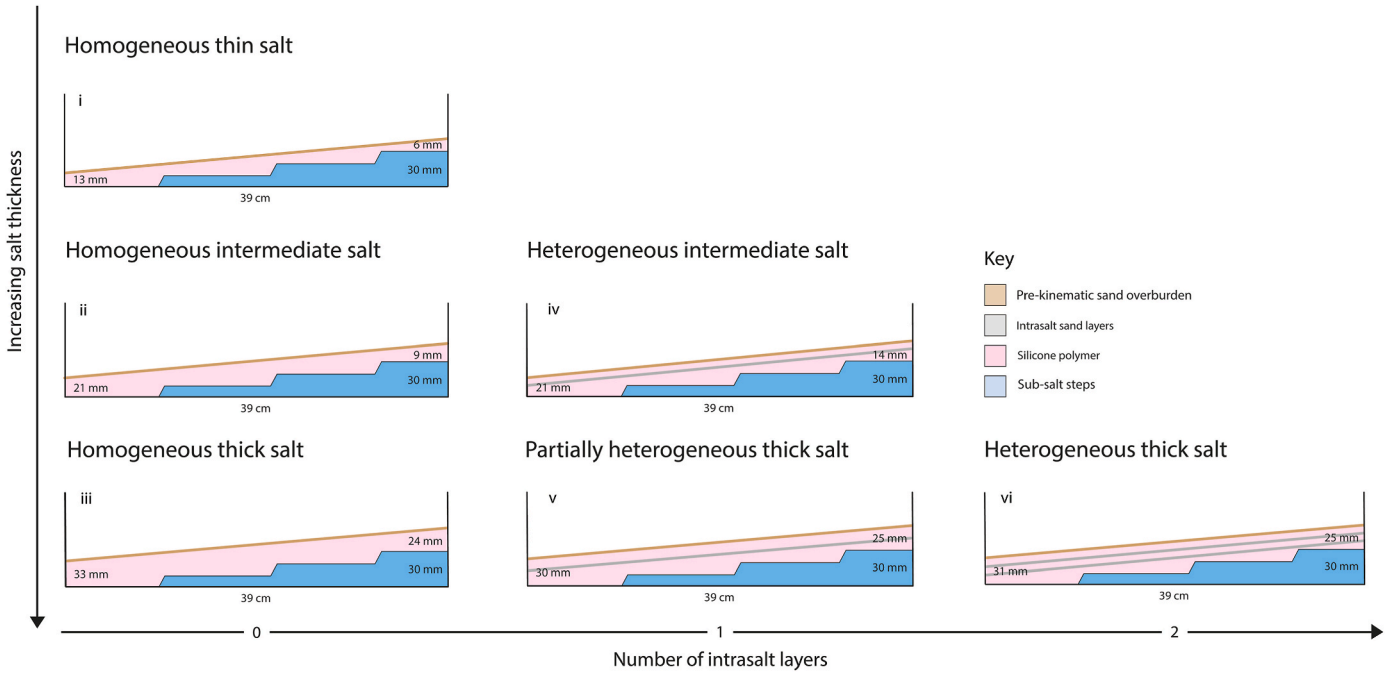

Fig. 3. Initial set-up of six physical analogue models with variable silicone thicknesses and intra-silicone heterogeneity. Models i) homogeneous thin salt, iii) homogeneous thick salt, and vi) heterogeneous thick salt are end-member model set-ups. All models comprise silicone thickening downdip and start with a thin pre-kinematic sand overburden (4 mm). Heterogeneous models comprise 4 mm thick intra-salt sand layers.

Table 1
Dynamic scaling parameters used in physical analogue models.

Quantity	Model	Nature	Ratio
Distance (m)	1	10^{5}	10^{-5}
Overburden density (kg·m−3)	1500–1700	2300	0.65–0.74
Overburden coefficient of friction	0.7	0.8	0.88
Salt density (kg·m^{-3})	987	2200	0.44
Salt viscosity (Pa·s)	$5{\cdot}10^{4}$	$5{\cdot}10^{19}$	10^{-15}
Gravity (m·s^{-2})	9.81	9.81	1
Time (s)	1	$8.76{\cdot}10^{9}$	$1.1{\cdot}10^{-10}$

Table 2
Variable parameters used for each model run (total thickness of the viscous salt analogue and number of brittle intra-silicone layers). All other parameters and boundary conditions were kept constant.

Model	Total salt thickness (mm) (updip – downdip)	Number of intra-silicone layers
Homogeneous thin salt	6–13	0
Homogeneous intermediate salt	9–21	0
Heterogeneous intermediate salt	16–21	1
Homogeneous thick salt	24–33	0
Partly-heterogeneous thick salt	29–34	1
Heterogeneous thick salt	25–31	2

comparable scale to that considered in the seismic reflection-based study of the Kwanza Basin, offshore Angola, in Evans and Jackson (2020), rather than modelling the entire kinematically-linked gravitational system from the shelf edge to the deep basin. We therefore use a scaling factor of 1 cm: 1 km, with a model width (along-strike) of 36 cm (c. 36 km) and length (across-strike) of 39 cm (c. 39 km) (Fig. 2).

To identify suitable analogue model materials, the rheologies of the natural rock types involved (i.e. clastic sediments and salt) must be constrained. Natural salt viscosities are variable, depending on several factors including composition, grain size, differential stress, temperature and fluid presence, but generally fall within the range 10^{15}–10^{19} Pa s (Jackson and Hudec, 2016; Schléder and Urai, 2005; Schléder et al., 2007; Spiers et al., 1988; Spiers and Carter, 1998; Urai et al., 1986, 2008). In this study, a silicone polymer (polydimethylsiloxane SGM-36) with a viscosity of c. 10^{4} Pa s was selected to represent the viscous salt layer, as is commonly used in salt modelling studies. If we consider that a reasonable viscosity for halite-dominated salt layers in the subsurface with moderate grain size and fluid presence is 10^{19} Pa s (Jackson and Hudec, 2016; Urai et al., 2008), this sets the time scaling factor as 1 h in the model representing approximately 1 Myr in nature.

Granular materials such as sand may be regarded as a continuous medium (prior to fault propagation) if the mechanics are studied at a scale much larger than that of the grain size, thus approximating the bulk mechanical properties of a natural clastic overburden (Nettleton and Elkins, 1947; Weijermars et al., 1993). Using sand to model a brittle overburden deforming above a ductile substratum has four main advantages: finite shear strength, brittle mode of deformation, low cohesion, and the ability to simulate syn-kinematic sedimentation (Weijermars et al., 1993; Koyi, 1997; Vendeville et al., 2002). In this study, alternating layers of fine sand and pyrex particles, both with a grain size of 100 μm, were used to represent clastic sedimentary layers in the overburden and brittle intra-salt layers.

2.3. Boundary conditions

The silicone was applied with the base-salt model back-tilted to resemble the initial post-rift basin geometry, such that the mobile unit thickens uniformly over each step toward the downdip end of the model. The silicone was left to settle for a minimum of 24 h after application to ensure cohesion, degassing and a smooth surface prior to each experiment. A pre-kinematic overburden (4 mm; c. 400 m) was added prior to model initiation, scaled to be broadly equivalent to the minimum thickness of the pre-kinematic Albian interval identified offshore Angola (e.g. Lundin, 1992; Duval et al., 1992; Hudec and Jackson, 2004; Evans and Jackson, 2020). Deformation was then induced by tilting the model forward to initiate gravity gliding from the updip end of the model to the

downdip end. The initial configurations and starting positions of each model are shown in Fig. 3.

Ramp syncline basins in the Kwanza Basin record more than 20 km of downdip translation (Hudec and Jackson, 2004; Evans and Jackson, 2020). Models were tilted by 1° in the initial stages and increased to 3° approximately halfway through the model duration, following other models of salt tectonic systems driven by gravity gliding (e.g. Ge et al., 2019). This reflects the progressive tilting of natural basin margins caused by post-rift subsidence in the deep basin and uplift of the continental margin (e.g. Hudec and Jackson, 2004). Syn-kinematic sedimentary layers were added as the model developed, infilling basin topography to create growth strata in the overburden. Sedimentary layers were applied with minor downdip thinning, but lateral uniform distribution, to reflect realistic thickness changes across the designated length-scale. Since we are modelling a relatively narrow portion of a much wider margin, we cut the model at the downdip end at regular time intervals to allow continued extension and translation over the steps, therefore simulating an 'open-toe' salt-tectonic system (cf. Gaullier et al., 1993; Dooley et al., 2017).

In total we conducted six experiments with basal steps (Fig. 3; Table 2). We varied the initial thickness and heterogeneity of the silicone layer for each experiment, and kept all other physical parameters and boundary conditions constant between experiments to isolate the effects of the chosen variables on the structural evolution. The minimum updip silicone thickness and maximum downdip silicone thickness for each experiment are reported in Table 2, along with the number of intra-silicone layers. We use fine sand to represent dominantly brittle intra-salt layers interbedded with halite-dominated mobile evaporites, as encountered in many salt-bearing sedimentary basins (e.g. Cartwright et al., 2012; Jackson et al., 2015; Warren, 2016; Rowan et al., 2019).

The experiments were performed in a CT scanner, which images the internal structure of the models during deformation. The density contrasts between the silicone, sand and pyrex are sufficient for them to be distinguished in CT imaging. This approach allows us to analyse the 3D internal structural development of the model as it evolves (c.f. Colletta et al., 1991; Adam et al., 2013; Zwaan and Schreurs, 2017), in contrast to traditional physical modelling approaches that permit only analysis of the model top or base during its evolution. Such models must be sliced open after they have run to completion to reveal their internal structure (e.g. Dooley et al., 2017), whereas the CT scanning approach is non-destructive. Analysis of the evolution of the analogue models can then be used to constrain tectono-stratigraphic interpretations of natural salt-tectonic systems identified in seismic reflection data. Our models provide unique insight into how structures evolve in 4D, enabling a full interpretation of the extent to which basal relief controls the distribution and style of overburden structures for different salt thicknesses and intra-salt heterogeneities. The edges of the model were excluded from the final analysis to remove boundary effects.

3. Model results

Here we describe the results of the three end-member models designed to investigate natural scenarios involving homogeneous thin salt (Fig. 3-i), homogeneous thick salt (Fig. 3-iii), and heterogeneous thick salt (Fig. 3-vi). The other three models are hybrid set-ups and were designed to support interpreted differences between the end-member models. The hybrid models therefore investigate scenarios involving homogeneous intermediate thickness salt (Fig. 3-ii), heterogeneous intermediate thickness salt (Fig. 3-iv) and partially heterogeneous thick salt (Fig. 3-v).

3.1. Homogeneous thin salt model

Immediately after translation begins in response to tilting, the model with a homogeneous, thin initial silicone layer (Fig. 3-i) develops three linear depocentres (with pre-kinematic layer at the base) parallel to, and directly downdip of, each basal step (Fig. 4a–i, 5a-i and 6a-i). The syn-kinematic sediments thicken into these depocentres and onlap the pre-kinematic layer. This leads to the development of three basins adjacent to each of the basal steps (Fig. 4a–ii). As gravity-driven downdip translation continues, the syn-kinematic strata are progressively rotated (in cross sectional view) and migrate downdip, while the location of the active depocentre remains immediately adjacent to the step.

As the basins thicken and subside with addition of growth strata, the underlying silicone thins in the vicinity of the step, increasing the basal friction (Fig. 4a–iii and 7a). As a result, the thicker silicone downdip of the depocentre moves at a greater velocity than the thinner silicone immediately adjacent to the step, causing extension in the overburden and the formation of graben structures at the downdip edge of each depocentre (Fig. 4a–iii, 6a-i and 7a). The grabens develop first at the end of the model where the steps are closest together, and rapidly propagate across the model following the strike of the associated step (Fig. 6a–i and 6a-ii). The stretched and thinned overburden within the grabens creates space into which the loaded silicone can flow, forming three linear reactive diapirs parallel to, and downdip of, each basal step (Fig. 4a–iv and 5a-ii). The asymmetric subsidence also creates monoclinal folds in the overburden directly above each step (Fig. 4a–v and 6a-ii). At the updip edge of the model, a graben opens adjacent and parallel to the model boundary where the overburden is pulling away (Fig. 6a–i and 6a-ii). This is considered a model edge effect.

As translation and sedimentation continue, the basins thicken and widen, and the reactive silicone diapirs continue to accommodate extensional strain by widening as they migrate downdip (Fig. 4a–v, 5a-iii and 6a-iii). When the diapirs translate across the next downdip step, their downdip flanks subside rapidly over the step, generating a pronounced asymmetry in the overburden (Fig. 8). This transforms the initially symmetrical grabens into half-graben style basins that are bound on their updip sides by normal faults located directly above the basal step (Fig. 8). The diapirs then collapse completely due to stretching as they translate over the step into the original depocentre, where they eventually become buried (Fig. 8), leaving little or no expression of the structure in plan view (Fig. 5a–iii and 6a-iii). This collapse occurs first at the edge of the model where the steps are more closely spaced, while the diapirs continue to grow and translate at the opposing edge of the model where the steps are more widely spaced (Fig. 5a–iii and 6a-iii). Eventually the basins subside to the point that they are effectively welded against the model base, but continue to translate slowly (Fig. 4a–vi). The updip basin is the first to weld, as this is where the silicone layer was initially (i.e. depositionally) thinnest, followed by sequential welding of the downdip basins.

The final structure of the model shows a clear relationship between the underlying basal steps and the distribution and orientation of the overburden structures. Even in the late stages of the model, the expression of the underlying steps is clear on the top-silicone and overburden surfaces, with all dominant structures (i.e. faults, reactive diapirs, basins and grabens) trending parallel or sub-parallel to the adjacent updip step (Fig. 5a–iii and 6a-iii). The model representing homogeneous thin salt therefore demonstrates a strongly coupled system where the sub-salt structure has a tangible influence on the supra-salt structural development.

We measure total translation by tracking the position of the two major silicone diapirs as the model evolves (Fig. 4a–vi). The distance from the original position of the updip diapir to its final position reveals c. 5 cm (equivalent to 5 km) of downdip translation, whereas the downdip diapir records c. 6 cm (equivalent to 6 km) of translation, which in turn indicates 1 cm (equivalent to 1 km) of cumulative syn-kinematic extension between the diapirs.

3.2. Homogeneous thick salt model

In this section we describe the development of the model representing homogeneous thick salt (Fig. 3-iii). The early stages of the

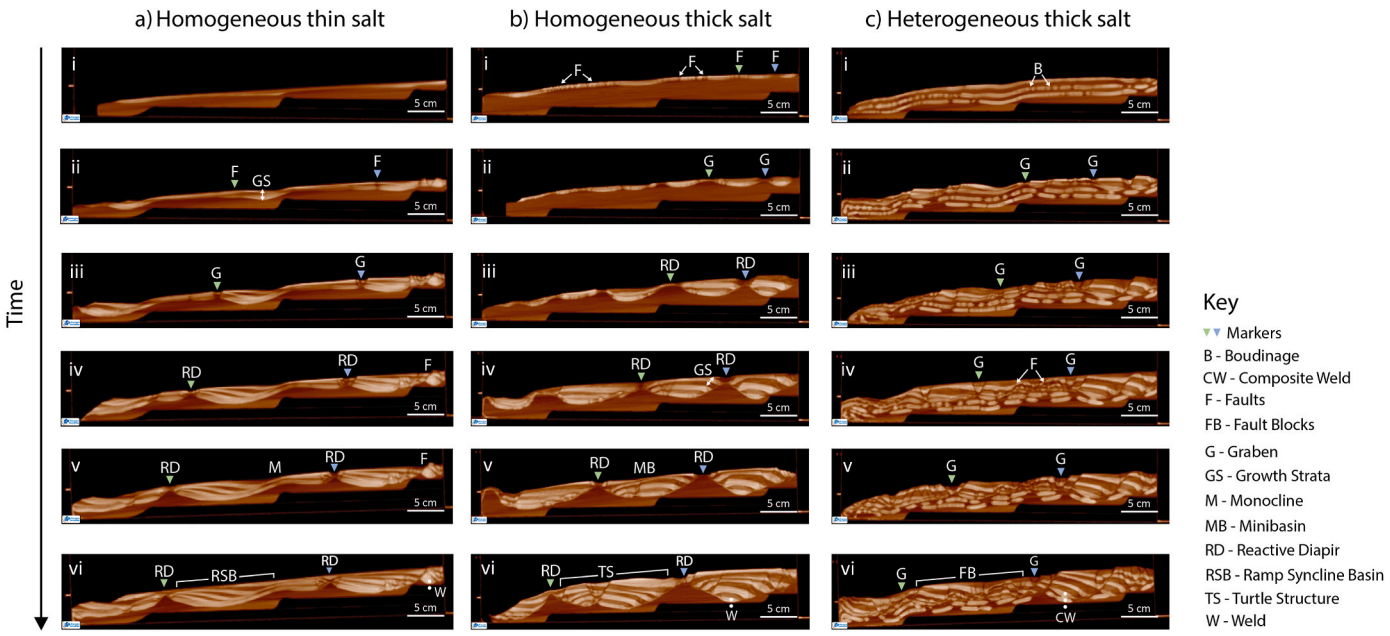

Fig. 4. CT-scan cross sections through physical analogue models showing the structural evolution of a) thin, b) thick and c) heterogeneous end-member salt models. The set-ups of these models are shown in Fig. 3 as i), iii) and vi) respectively. The homogeneous thin salt model develops reactive diapirs and ramp syncline basins. The homogeneous thick salt model develops reactive diapirs and turtle minibasins. The heterogeneous thick salt model develops boudinaged intra-silicone layers, overburden fault blocks and composite welds. The blue and green triangular markers track the position of selected structures in order to measure total translation and extension across the model. Key features are annotated. (For interpretation of the references to colour in this figure legend, the reader is referred to the Web version of this article.)

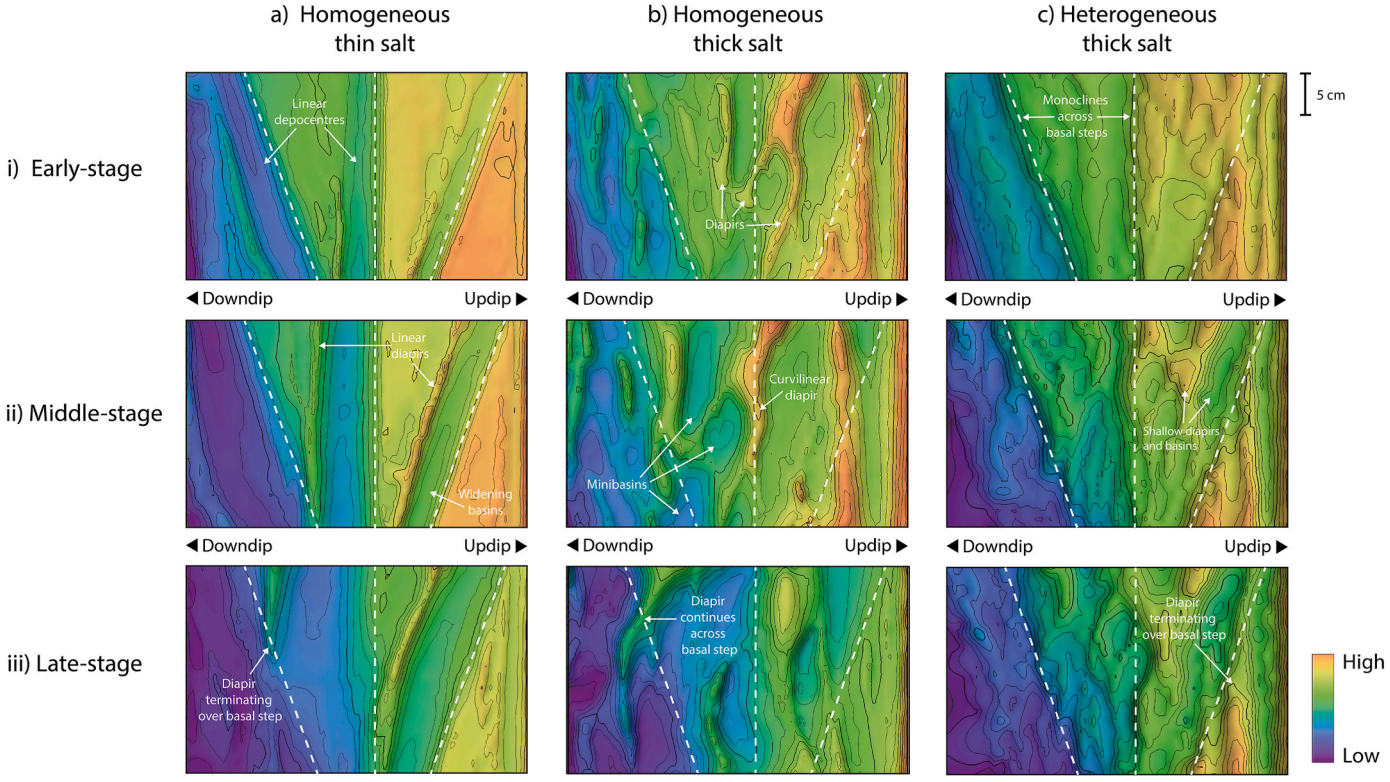

Fig. 5. Plan-view elevation of the top-silicone surface for a) thin, b) thick and c) heterogeneous salt models imaged at 3 stages during model evolution. The set-ups of these end-member models are shown in Fig. 3 as i), iii) and vi) respectively. Dashed white lines indicate location of underlying steps at model base. Note that in all images the edges of the model have been cut to eliminate the boundary effects.

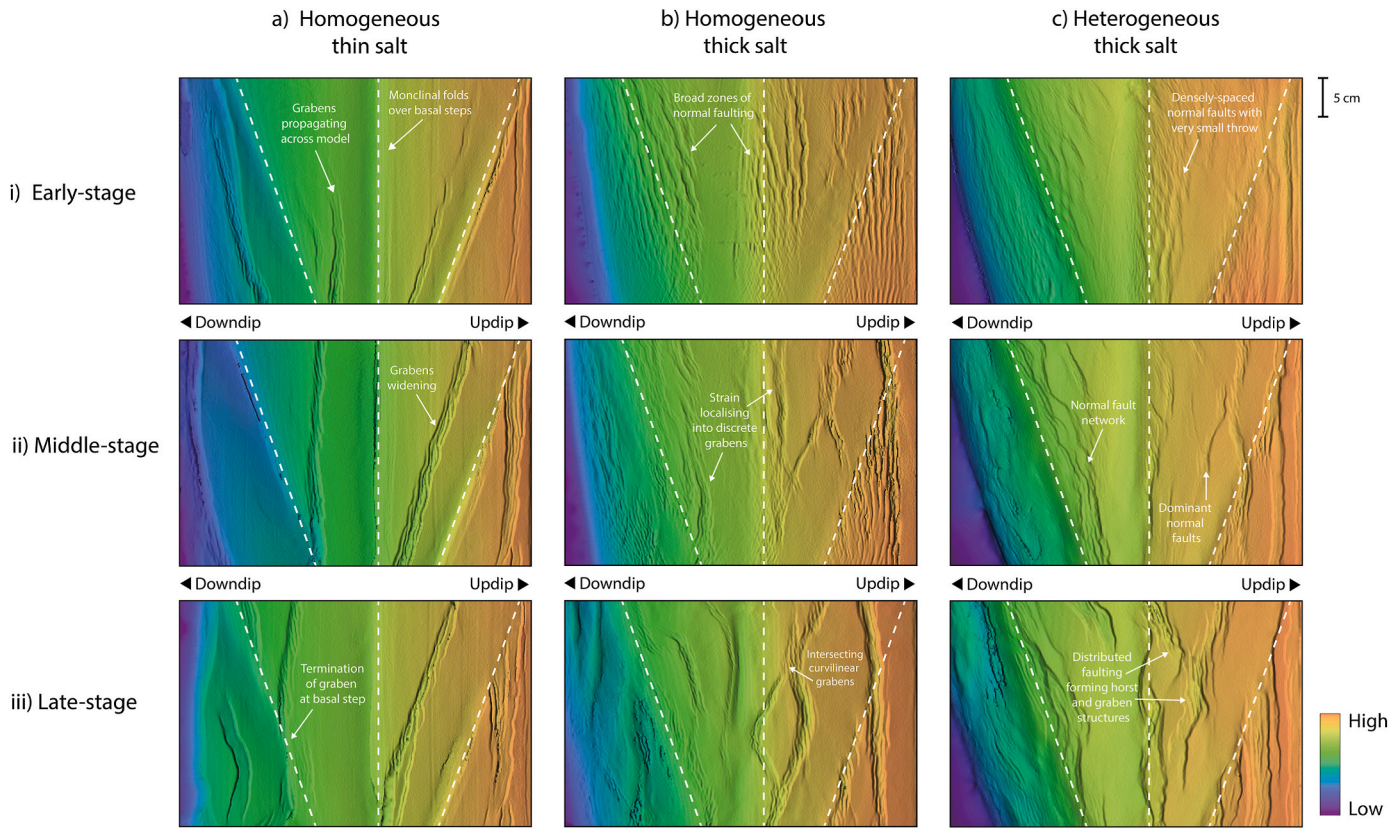

Fig. 6. Plan-view elevation of the model surface for a) thin, b) thick and c) heterogeneous salt models imaged at 3 stages during model evolution. The set-ups of these end-member models are shown in Fig. 3 as i), iii) and vi) respectively. Dashed white lines indicate location of underlying steps at model base. Note that in all images the edges of the model have been cut to eliminate the boundary effects.

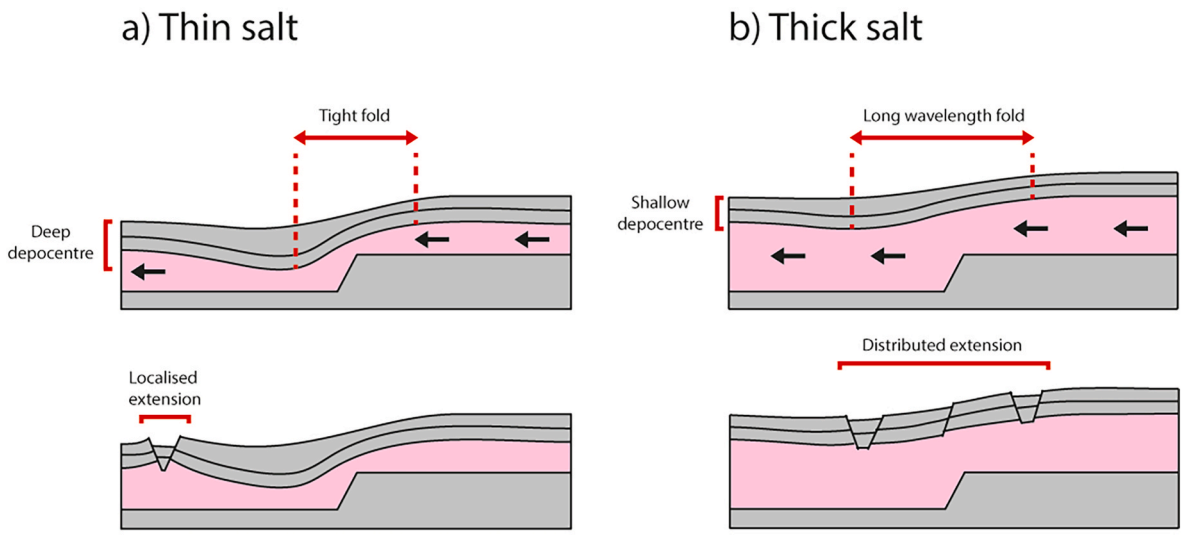

Fig. 7. Schematic diagram highlighting key differences between the early-stage development of the a) homogeneous thin salt, and b) homogeneous thick salt models. The set-ups of these models are shown in Fig. 3 as i) and iii) respectively. In the thin salt model, the flux imbalance across the step creates a deep RSB depocentre, increasing basal friction adjacent to the step and localising the extensional strain downdip. In contrast, there is little flux imbalance across the step in the thick salt model, consequently the RSB depocentre is shallow and strain more evenly distributed.

homogeneous thick salt model show widely distributed overburden extension (Fig. 4b–i, 6b-i and 7b). The extension is accommodated by a population of normal faults with very small throws spread across a wide surface area (Fig. 4b–i, 6b-i and 7b). In the middle and at the downdip end of the model, these faults form above, and strike parallel to, the basal steps (Fig. 6b–i). In contrast, at the updip edge of the model where the overburden is pulling away from the model boundary, the faults are oblique to the underlying step and instead trend parallel to the model boundary (Fig. 6b–i). This could be considered a model edge effect. However, these faults terminate laterally over the edge of the step, such that the underlying step is still expressed at the model surface (Fig. 6b–i). This broadly distributed extension differs from the thin salt

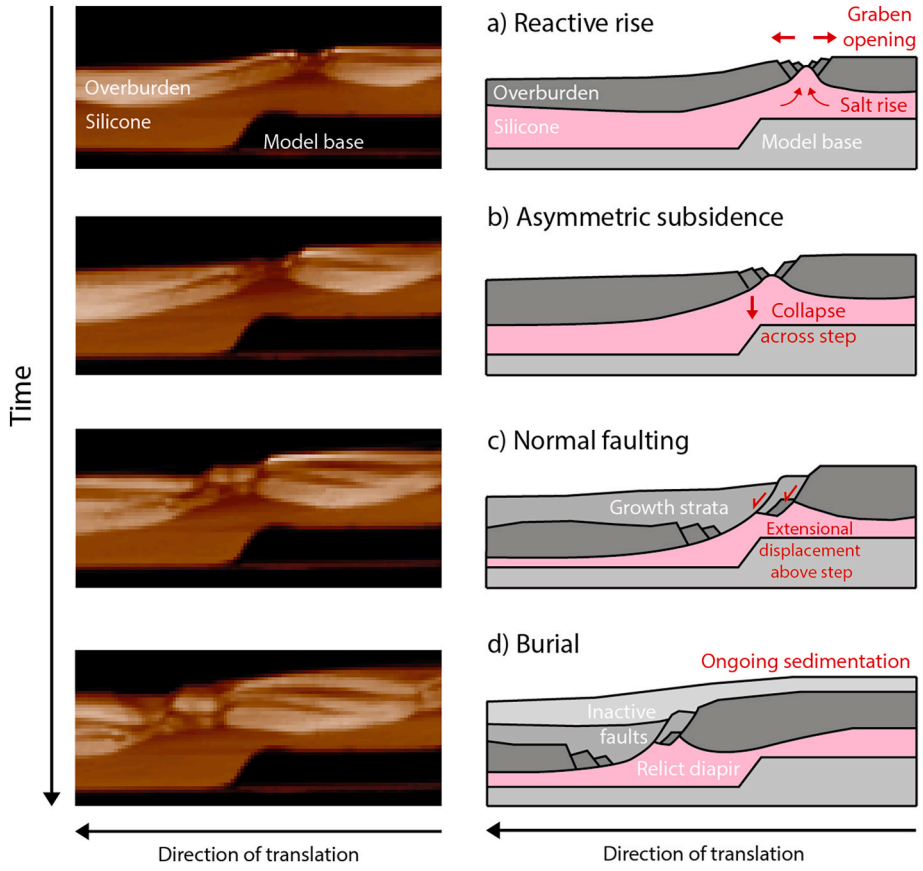

Fig. 8. Zoom-in CT-scan cross sections of the homogeneous thin salt model evolution paired with schematic illustrations showing diapir collapse due to extension as the diapir is translated across the basal step. The set-up of this model is shown in Fig. 3 as i).

model, where extension in the overburden is localised very early in the model evolution, leaving the rest of the overburden relatively undeformed.

As translation continues and the overburden thickens, strain localises into discrete grabens and many of the initial small faults become inactive and buried (Fig. 4b–ii and 6b-ii). As observed in the thin salt model, this localised extension leads to the development of reactive diapirs (Fig. 4b–iii and 5b-i). Syn-kinematic sediments thicken across the crests of the diapirs, and listric normal faults along the flanks accommodate continued extension (Fig. 4b–iv). Displacement on these faults causes downward rotation of the strata adjacent to the flanks, creating minibasins with antiformal internal geometries (Fig. 4b–v). Note that these anticlines are extensional in origin and form prior to welding. The broad, triangular diapirs separating the minibasins are oriented sub-perpendicular to the translation direction and have a curvilinear geometry in plan view (Fig. 5b–ii).

As the diapirs move over the next downdip basal step, they subside asymmetrically, in a similar manner to that observed in the thin salt model (Fig. 4b–vi). However, in this case they do not collapse completely, but instead continue to widen when they reach the next flat between steps. By the late stage of the model, there is no longer a clear spatial relationship between the distribution and trend of structures in the overburden and the steps (Fig. 5b–iii). Rather than being aligned with the underlying steps, dominant structures are oriented perpendicular or sub-perpendicular to the translation direction (Fig. 5b–iii and 6b-iii). The final structure of the model does not bear a clear spatial resemblance to the geometry of the basal surface, representing a very weakly coupled or decoupled system (Fig. 5b–iii and 6b-iii).

We track the position of the two dominant diapirs during the model evolution to calculate the magnitude of horizontal translation (Fig. 4b–vi). The distance from the original position of the updip diapir to its final position reveals c. 12 cm (equivalent to 12 km) of downdip translation, whereas the downdip diapir reveals a significantly larger magnitude of c. 23 cm (equivalent to 23 km) of translation. This indicates 11 cm (equivalent to 11 km) of cumulative syn-kinematic extension between the diapirs. Both the total magnitude of translation and the magnitude of extension are therefore larger than observed in the thin salt model.

3.3. *Heterogeneous thick salt model*

Here we describe the evolution of the model representing thick, heterogeneous salt, which comprises two sand layers encased within silicone (Fig. 3-vi). As gliding initiates, the early stages of the heterogenous model show distributed strain in the overburden, similar to the distribution observed in the early stages of the homogeneous thick salt model but more diffuse (Fig. 4c–i and 6c-i). Monoclinal folds form above each of the steps and the sand layers encased within the silicone begin to boudinage as they stretch (Fig. 4c–i).

Grabens develop in the overburden, as observed in the homogenous models, but the encased sand layers restrict the flow of mobile silicone from feeding into reactive diapirs and inhibit subsidence of the adjacent basins (Fig. 4c–ii and 6c-ii). This means that strain does not localise within discrete diapiric structures but remains diffuse, and the top-silicone surface therefore shows little variation in the height of relief compared to the homogeneous models (Fig. 5c–i and 5c-ii). The lateral translation of the overburden across the basal steps creates depocentres adjacent to each step, which accommodate growth strata in a similar manner to that observed in the thin salt case described previously (Fig. 4c–iii and 6c-ii).

However, the lack of strain localisation means that these step-parallel basins are frequently dissected by normal faults (Fig. 4c–iv).

The normal faults with the largest displacements dip toward the downdip end of the model and are associated with a number of synthetic and antithetic faults, resulting in complex patterns of growth strata in the hangingwall (Fig. 4c–v).

During translation the thin, mobile silicone layers are evacuated in several places, creating discontinuous primary welds where the overburden touches down onto the intra-silicone boudins (Fig. 4c–v). In some locations these become stacked composite welds where the intra-silicone boudins are discontinuously welded to each other or the base of the model (Fig. 4c–v). In the updip domain, where the boudins have been displaced from beneath a subsiding fault block, the overburden is almost directly welded to the base of the model (Fig. 4c–v).

The final structure of the model is therefore dominated by normal faults that give rise to a series of displaced overburden blocks discontinuously welded to the boudinaged intra-silicone layers (Fig. 4c–vi). The orientation and distribution of overburden structures show a broad relationship with the basal steps, with some structures trending approximately sub-parallel to the underlying step, though most are oriented sub-perpendicular to the translation direction (Fig. 5c–iii and 6c-iii). The heterogeneous thick salt model shares some characteristics with both the homogeneous thick and thin salt models, but is distinct from either in that the overburden is characterised by internally complex fault blocks.

Tracking the position of two major structures as the model evolves shows c. 7 cm (equivalent to 7 km) of horizontal translation in the updip domain and c. 15 cm (equivalent to 15 km) of translation in the downdip domain, indicating 8 cm (equivalent to 8 km) of cumulative syn-kinematic extension across the model. These magnitudes of translation and extension are intermediate between the thin salt model and homogeneous thick salt model.

3.4. Hybrid models

In addition to the three end-member models described above, we also ran three models representing hybrid set-ups: homogeneous salt with intermediate thickness (Fig. 3-ii), heterogeneous salt with intermediate thickness (Fig. 3-iv), and a partially heterogeneous thick salt model (Fig. 3-v). Having described the evolution of the end-member models in detail above, here we discuss the final structures of the hybrid models to facilitate comparison of the end members (Fig. 10). The hybrid models allow us to better understand the behaviours of the end-member models and isolate important differences between the models.

The homogeneous, intermediate thickness salt model is a hybrid between the homogeneous thin salt and homogeneous thick salt end-member models (Fig. 3-ii and 10-ii). The intermediate model develops triangular reactive diapirs, as observed in both end-member models, separated by growth wedges that thicken updip and terminate against diapir flanks or downdip-facing normal faults (Fig. 10). If instead the growth wedges upturned and onlapped the updip strata, the basins would be more structurally similar to the homogeneous thin salt end-member model. In contrast, greater displacement on the opposing diapir flank would generate antiformal minibasins similar to those observed in the homogeneous thick salt end-member. The final overburden structure of the intermediate model therefore shares distinct hybrid features with its end-members. However, the overall blocky, fault-dominated structure is most similar to that produced in the heterogeneous thick salt model, but with fewer and more widely spaced structures, indicating a greater degree of strain localisation (Fig. 10).

The partially heterogeneous thick salt model contains a single intra-silicone layer, representing a hybrid between the homogeneous thick salt and heterogeneous thick salt end-member models (Fig. 3-v and 10-v). The final structure of the hybrid model comprises a broad reactive diapir similar to the homogeneous model, as well as graben structures underplated by intra-silicone stringers, as observed in the heterogeneous model (Fig. 10). The growth strata are again dominantly thickening and dipping toward the updip end of the model due to greater displacement on the downdip flank of the diapir and the dominance of downdip-facing normal faults. However, the extensional faulting is not as densely spaced and broadly distributed as in the fully heterogeneous model, indicating increased strain localisation (Fig. 10).

The heterogeneous intermediate thickness salt model is a hybrid between the homogeneous thin salt and heterogeneous thick salt end-member models (Fig. 3-iv and 10-iv). No reactive diapirs are developed in the hybrid model and the overburden is instead segmented by grabens and normal faults dipping toward the downdip end of the model, with updip-thickening growth strata. In this case the final structure of the hybrid model more closely resembles the heterogeneous thick salt model and shares fewer characteristics with the homogeneous thin salt model. The distribution and density of faulting is similar in both the hybrid model and the heterogeneous end-member model, indicating a lack of strain localisation in both cases. In the following section we discuss the factors controlling the observed similarities and differences between the models.

4. Discussion

Gravity gliding and spreading are the dominant driving mechanisms of salt tectonics on many salt-bearing passive margins (Schultz-Ela, 2001; Rowan et al., 2004, 2012; Brun and Fort, 2011; Peel, 2014). However, both processes are commonly associated with the basinward flow of homogeneous salt across a smoothly basinward-dipping base-salt surface (e.g. Jackson et al., 1994; Schultz-Ela, 2001; Brun and Fort, 2011; Peel, 2014; Allen et al., 2016), overlooking the important roles of base-salt relief and salt rheology in controlling intra-salt and supra-salt kinematics, and the resultant structural style. The physical models presented here highlight the structural complexity introduced by the interplay between base-salt relief, salt thickness and intra-salt lithological heterogeneity during gravity-driven salt tectonics. Here we discuss the key findings derived from the models and compare our observations to seismic reflection-based studies of natural salt-bearing sedimentary basins.

4.1. Salt thickness

The structural evolution of the homogeneous thin salt and thick salt models differ significantly, despite the experimental setup, and physical parameters other than silicone thickness, being kept constant (Fig. 4). In the thin homogeneous salt model, the continuous lateral translation of the overburden across the basal steps led to the development of local basins adjacent to each step, which are similar to natural examples found on salt-influenced margins known as ramp syncline basins (RSBs) (Fig. 4a–vi). RSBs form when salt flows over relief on a base-salt surface, creating local accommodation that preserves landward-dipping and -thickening growth strata (Hudec and Jackson, 2004; Jackson and Hudec, 2005; Dooley et al., 2017; Dooley et al., 2018; Pichel et al., 2018; Evans and Jackson, 2019; Rowan et al., 2022). The RSBs that developed in the thin salt model resemble those identified from seismic studies of the Kwanza Basin offshore Angola, the Santos Basin offshore Brazil, and on the Levant margin offshore Lebanon (Jackson and Hudec, 2005; Pichel et al., 2018; Evans and Jackson, 2019; Evans et al., 2020; Rowan et al., 2022). A low ratio of salt thickness to base-salt relief increases the coupling between supra-salt and sub-salt structures, and thus promotes RSB development.

RSBs record, and therefore allow us to measure, the minimum magnitude of salt-detached translation. This means that we can reconstruct the updip positions of translated salt structures on the margin, and in doing so unravel some of the structural complexity in the context of salt flow interaction with base-salt relief. The well-defined RSBs developed in the thin salt model allow direct measurement of translation distance over each basal step from its final structural configuration, using the distance from the first intra-RSB onlap to the most recent

(Fig. 4a). In the homogeneous thick salt model, however, it would be difficult to constrain the magnitude of translation from its final structure, because we do not have any constraints on the initial positions of the structures we observe (Fig. 4b). However, tracking the position of diapirs through time during model evolution demonstrates that a significant amount of downdip translation has occurred (Fig. 4b). This means that even in salt tectonic systems where no RSBs or other direct indicators of lateral translation have been identified, the supra-salt structures may still have been translated a significant distance downdip. This information is pertinent to petroleum systems analysis because it may affect the charge of supra-salt trap structures if we assume vertical migration of fluids from the sub-salt.

The antiformal minibasins that developed in the homogeneous thick salt model closely resemble well-documented structures in natural salt basins known as turtle anticlines (Fig. 4b–vi) (Trusheim, 1960; Duval et al., 1992; Lundin, 1992; Mauduit et al., 1997). The turtle anticlines that developed in the model formed due to extension between diapirs. Classic turtle structures (Trusheim, 1960) form due to minibasin subsidence and inversion during welding, and are not traditionally extensional in origin. Extensional turtle structures, such as those developed in the model presented here, are similar in geometry but not in process (Vendeville and Jackson, 1991; Jackson et al., 1994). In this case the subsidence of the anticline flanks is facilitated by normal faulting. Turtle structures have been described from seismically-imaged examples found offshore Gabon and Angola, in the Campos Basin offshore Brazil, and in the Gulf of Mexico (Mauduit et al., 1997; Demercian et al., 1993; Jackson and Hudec, 2016; Dooley et al., 2017). Such structures were prevented from forming in the thin salt and heterogeneous salt models due to the lack of mobile silicone to feed widening diapirs, and may be indicative of weak coupling between supra-and sub-salt structures.

Thicker salt promotes a greater component of vertical motion (overburden subsidence and diapir rise) as well as overall lateral motion, whereas thin salt systems are largely dominated by lateral motion with only a minor component of vertical motion. Thick salt models are also characterised by faster translation rates and larger magnitudes of translation (as they do not weld as quickly). Overall, the thin salt model shows a much greater degree of coupling between the basal steps and overburden structures, indicating strong control of the basal geometry on the silicone flow and overburden kinematics (Figs. 5 and 6). By contrast, the final structure of the thick salt model is dominated by overburden structures oriented sub-perpendicular to the direction of gliding, and that show a greater degree of spatial decoupling from the basal structures, indicating a much weaker influence of the basal steps (Figs. 5 and 6).

Note that the observed differences in overburden structural style do not relate to absolute salt thickness, but rather the ratio between salt thickness and base-salt relief. Where the ratio is low (i.e. salt is thin relative to the height of relief), the geometry of the base-salt has a significant impact on the subsequent structural evolution of the salt and overburden. The spatial variations in volumetric flux and flow velocity, generated by salt flow over the base-salt steps, control the distribution and orientation of supra-salt depocentres and structures, thus resulting in strong coupling. Where the ratio is high (i.e. salt is much thicker than the height of relief), these variations in salt flux are less pronounced and therefore the resulting overburden deformation is only weakly coupled to the base-salt relief. This is consistent with the findings of previous studies that have demonstrated increased mobile salt thickness promotes greater decoupling in both thick-skinned tectonic settings (e.g. Withjack and Callaway, 2000; Miró et al., 2023; Ferrer et al., 2023) and purely gravity-driven systems (e.g. Stewart et al., 1997; Dooley et al., 2017; Roma et al., 2018). In the homogenous thin and homogeneous thick salt models presented here this ratio is approximately 1 and 3, respectively. The model results demonstrate that this ratio is a first-order control on the tectono-stratigraphic development of the overburden. This means that even basins with very thick salt deposits may show strong coupling between sub- and supra-salt structures if the magnitude of the base-salt relief is large enough.

Because both the salt thickness and the magnitude of relief vary spatially across individual basins, it is possible to have strongly coupled structures developing contemporaneously with weakly coupled structures in the same basin. Some parts of the basin may be characterised by a low ratio (i.e. the base-salt is highly rugose or the salt is thin, and therefore coupling is strong) whereas other parts may have a high ratio (i.e. the base-salt relief is very low or the salt is thick, and therefore coupling is weak). For example, both turtle anticlines and RSBs are found in the extensional and translational domains of the Kwanza Basin, offshore Angola (Hudec and Jackson, 2004; Evans and Jackson, 2020).

Structures may also be translated through domains of both high ratio and low ratio salt thickness to base-salt step height during their development. Structures developed updip with no influence from base-salt relief may be subsequently translated into an area with significant base-salt relief as the overburden translates basinward. We should therefore expect to see structural overprinting during different phases of translation as the system evolves, adding further complexity. Such overprinting has been inferred in natural salt systems such as the Kwanza Basin, offshore Angola (Jackson and Hudec, 2005; Evans et al., 2020; Erdi and Jackson, 2021) and observed in previous physical modelling studies (Dooley et al., 2017, 2020; Ge et al., 2019).

Finally, we note that the evolution of salt thickness through time can also affect the coupling of the system at different stages of translation, and introduce further structural overprinting. For example, the salt layer typically thins over time as it is extended (in the extensional domain) and/or moves into diapirs (anywhere on the margin). This decreases the ratio of salt thickness to height of relief and may therefore lead to a transition from a decoupled system to a more strongly coupled system. Furthermore, thick-skinned tectonic events may change the height of base-salt relief over time, for example by increasing the offset of basal normal faults if extension is ongoing, or even decreasing offset in the case of regional inversion. Such events would also cause temporal variations in the ratio of salt thickness to height of relief, and therefore increase or decrease the degree of coupling over time.

4.2. Salt heterogeneity

The addition of intra-silicone layers to the thick salt model increased the degree of coupling between the overburden structure and basal steps. By inhibiting vertical motion, the dominance of lateral translation caused depocentres in the overburden to form adjacent to the basal steps, as observed in the thin salt model (Fig. 4). However, the reduced vertical motion and lack of available mobile silicone also inhibited strain localisation and diapir growth, which resulted in distributed normal faulting across the model throughout its evolution (Fig. 9). This distributed faulting within the basins overprinted the landward-thickening trend typically characterising RSBs (Hudec and Jackson, 2004; Pichel et al., 2018; Evans and Jackson, 2019), resulting in greater structural complexity. Despite limited strain localisation, the orientation of the structures aligned more closely with the basal steps than those formed in the homogeneous thick salt model (Figs. 5 and 6). The final structure of the model is unique but shares some attributes with both the thin salt model and homogeneous thick salt model. A very similar evolution and resultant structural style was observed for the heterogeneous intermediate thickness salt model. This is likely due to the similar ratio of brittle-to-ductile materials in the heterogeneous thick salt model and heterogeneous intermediate thickness salt model (Fig. 3-iv and 3-vi).

Intra-salt heterogeneity is a result of spatial and temporal changes in the depositional environment (Tucker, 1991; Warren, 2016; Rodriguez et al., 2018). The lithological composition of evaporite sequences can therefore vary widely between different basins, depending on oceanographic conditions, basin physiography, and nature of clastic input, and can also vary across individual basins on relatively short length scales (Warren, 2016). This could explain some of the observed spatial variability in structural styles on salt-influenced passive margins. For

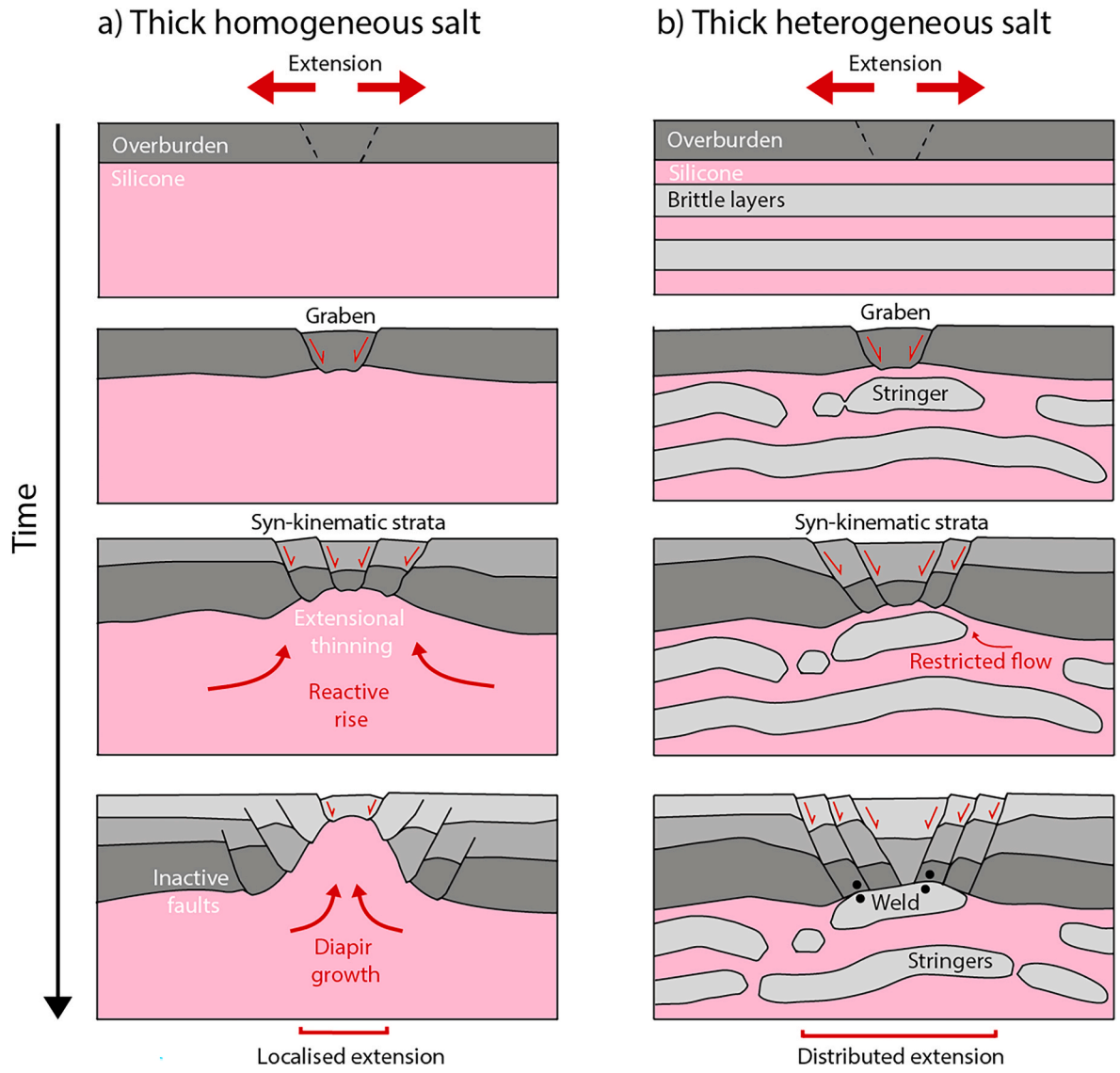

Fig. 9. Schematic illustration comparing extensional strain development in a) thick homogeneous salt, and b) thick heterogeneous salt models. The set-ups of these models are shown in Fig. 3 as iii) and vi) respectively. The thick homogeneous salt model promotes diapiric rise and localises strain within and above reactive diapirs, whereas the intra-salt layers in the heterogeneous salt model inhibit diapiric rise and strain remains more distributed.

example, salt walls develop locally at one part of the Levant margin but are absent elsewhere along the margin, despite the wide extensional domain (Evans and Jackson, 2021). Rheological variations may have inhibited diapiric development along most of the margin, but a local change in the mechanical stratigraphy or decrease in the bulk viscosity of the evaporite sequence may have favoured local reactive rise and salt wall development.

It is difficult to assess the impact of intra-salt heterogeneity in more mature basins, where salt tectonics is more advanced, due to limitations in seismic imaging, which gives poor constraints on the internal composition and deformation of the salt body. However, rare reflectivity is observed within the Aptian salt in the Santos Basin, offshore Brazil, and spatial variations in the structural style may be tentatively linked to lateral variations in the intra-salt composition (Jackson et al., 2015; Rodriguez et al., 2018; Pichel et al., 2020). A study of well penetrations in the Campos Basin, offshore Brazil, also supported a connection between the increasing thickness and proportion of halite in the deep basin and increased prevalence of diapiric structures, in contrast to the inboard portion of the margin where salt is thinner and intra-salt heterogeneity appears to have restricted vertical subsidence and diapiric rise (Wagner and Jackson, 2011). This is consistent with our modelling results and also implies that structures in the inboard portion of the margin should exhibit greater coupling with the base-salt relief.

4.3. *Wider implications*

Although conceptually based on observations of base-salt relief and supra-salt structures in the Kwanza Basin, offshore Angola (Evans and Jackson, 2020), the insights gained from analysis of the physical analogue models in this study reach much further, given that many other salt basins, such as the Gulf of Mexico and offshore Brazil, are also characterized by heterogeneous salt and/or rugose base-salt surfaces (e.g. Tucker, 1991; Cartwright et al., 2012; Jackson et al., 2015; Dooley and Hudec, 2017; Ferrer et al., 2017; Pichel et al., 2019b; Rowan et al., 2019; Evans and Jackson, 2021; do Amarante et al., 2021). These variables could at least partly explain why we observe contrasting styles of deformation in different salt basins around the world, and even on individual salt-bearing passive margins where gravitationally driven deformation is dominant. Many of the structures developed in the models, such as RSBs, turtle-back anticlines and reactive diapirs, closely

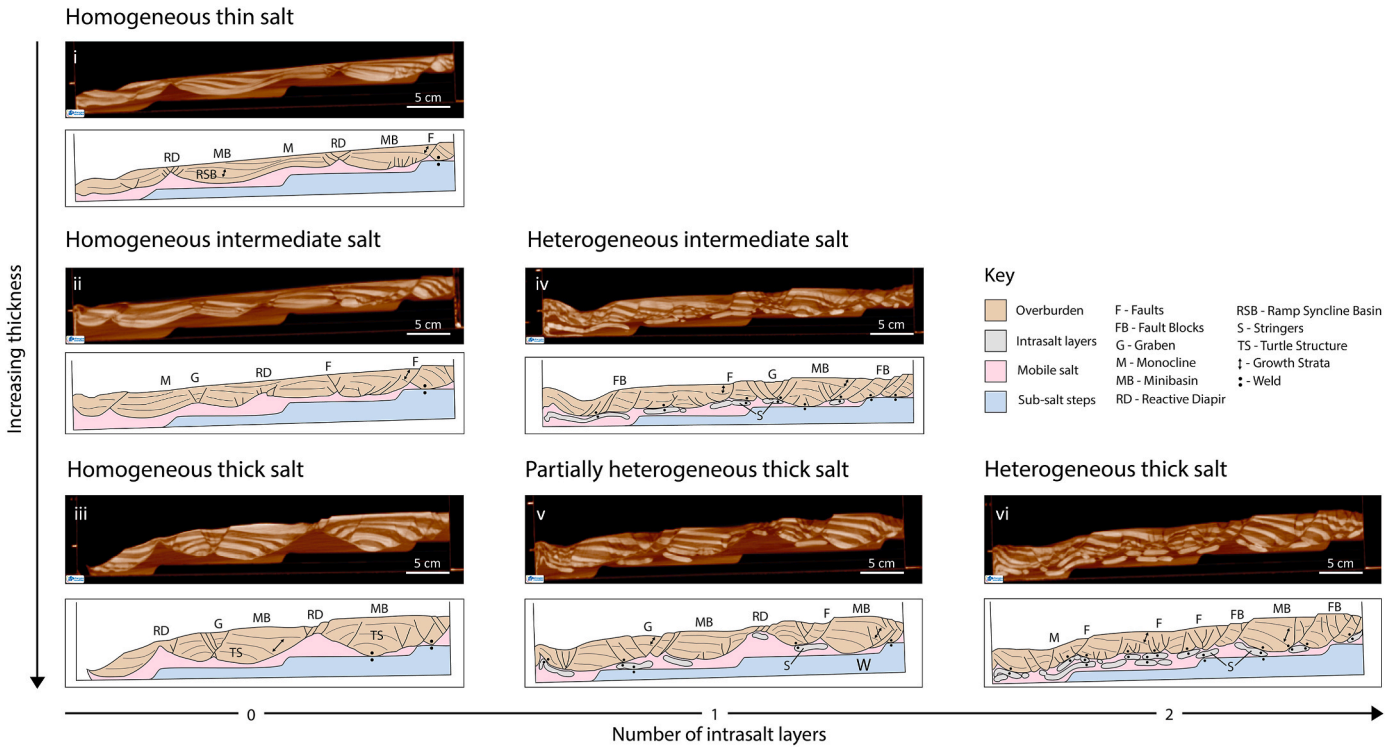

Fig. 10. CT-scan cross sections and illustrated interpretations showing the final structure of all models including end-member and hybrid scenarios. Key features are annotated.

resemble natural examples imaged in seismic data, highlighting important controls on their kinematic development. In subsurface exploration this will enable better assessment of the geometries and distribution of salt-related traps on salt-bearing margins, as well as constraining the timing of trap generation.

Whilst an undeniably powerful method, the physical modelling approach has intrinsic limitations which must be considered in light of all interpretations. The models presented here are inherently over-simplifications of natural systems, where base-salt geometries may be infinitely more complex and have many other variables at play, but by reducing the complexity of the system in this way we have succeeded in isolating the influence of certain parameters to further our understanding of specific geological processes. The models clearly show that the magnitude of base-salt relief relative to salt thickness, and mechanical stratigraphy introduced by intra-salt heterogeneity, are important first-order controls on the structural evolution of the basin, affecting both the types of structures developed and the extent to which supra-salt structures are coupled to the base-salt relief.

5. Conclusions

- The magnitude of salt thickness relative to the magnitude of base-salt relief is an important first-order control on supra-salt structural evolution during thin-skinned, gravity-driven salt tectonics in the proximal, extension-dominated portion of the margin.
- Low salt thickness to base-salt relief ratios result in strong coupling between the base-salt relief and supra-salt structure, characterised by ramp syncline basin development and salt walls/depocentres aligned with orientation of base-salt relief.
- High salt thickness to base-salt relief ratios result in weak coupling between the base-salt relief and supra-salt structure, characterised by extensional turtle anticlines and salt walls/depocentres oriented sub-perpendicular to the dominant translation direction.
- Intra-salt heterogeneity inhibits vertical movement and strain localisation, and promotes greater coupling with the base-salt relief.

CRediT authorship contribution statement

Sian L. Evans: Writing – review & editing, Writing – original draft, Methodology, Formal analysis, Conceptualization. **Christopher A-L. Jackson:** Writing – review & editing, Supervision, Methodology. **Sylvie Schueller:** Writing – review & editing, Methodology, Conceptualization. **Jean-Marie Mengus:** Methodology, Conceptualization.

Declaration of competing interest

The authors declare that they have no known competing financial interests or personal relationships that could have appeared to influence the work reported in this paper.

Data availability

Data will be made available on request.

Acknowledgements

The modelling work presented here was performed at IFP Energies Nouvelles in collaboration with the Basins Research Group at Imperial College London. Grateful thanks to Juliette Hello for assistance in the lab. The American Association of Petroleum Geologists and the Geological Society of London generously awarded grants to support this project. This work would not have been possible without the legacy of pioneering work on physical modelling by Bruno Vendeville, to whom this special issue is dedicated. We would also like to thank Tim Dooley and an anonymous reviewer for their constructive reviews which greatly improved the quality of the manuscript, as well as editor of the special issue Mark Rowan and the JSG editorial team.

References

Adam, J., Klinkmüller, M., Schreurs, G., Wieneke, B., 2013. Quantitative 3D strain analysis in analogue experiments simulating tectonic deformation: integration of X-

ray computed tomography and digital volume correlation techniques. J. Struct. Geol. 55, 127–149.
Allen, H., Jackson, C.A.L., Fraser, A.J., 2016. Gravity-driven deformation of a youthful saline giant: the interplay between gliding and spreading in the Messinian basins of the Eastern Mediterranean. Petrol. Geosci. 22 (4), 340–356.
Brun, J.P., Fort, X., 2011. Salt tectonics at passive margins: geology versus models. Mar. Petrol. Geol. 28 (6), 1123–1145.
Cartwright, J., Jackson, M., Dooley, T., Higgins, S., 2012. Strain partitioning in gravity-driven shortening of a thick, multilayered evaporite sequence. Geological Society, London, Special Publications 363 (1), 449–470.
Cobbold, P., Rossello, E., Vendeville, B., 1989. Some experiments on interacting sedimentation and deformation above salt horizons. Bull. Soc. Geol. Fr. (3), 453–460.
Colletta, B., Letouzey, J., Pinedo, R., Ballard, J.F., Balé, P., 1991. Computerized X-ray tomography analysis of sandbox models: examples of thin-skinned thrust systems. Geology 19 (11), 1063–1067.
Demercian, S., Szatmari, P., Cobbold, P.R., 1993. Style and pattern of salt diapirs due to thin-skinned gravitational gliding, Campos and Santos basins, offshore Brazil. Tectonophysics 228 (3–4), 393–433.
do Amarante, F.B., Jackson, C.A.L., Pichel, L.M., dos Santos Scherer, C.M., Kuchle, J., 2021. Pre-salt rift morphology controls salt tectonics in the Campos Basin, offshore SE Brazil. Basin Res. 33 (5), 2837–2861.
Dooley, T.P., Hudec, M.R., Pichel, L.M., Jackson, M.P., 2020. The impact of base-salt relief on salt flow and suprasalt deformation patterns at the autochthonous, paraautochthonous and allochthonous level: insights from physical models. Geological Society, London, Special Publications 476 (1), 287–315.
Dooley, T.P., Hudec, M.R., Carruthers, D., Jackson, M.P., Luo, G., 2017. The effects of base-salt relief on salt flow and suprasalt deformation patterns—Part 1: flow across simple steps in the base of salt. Interpretation 5 (1), SD1–SD23.
Dooley, T.P., Hudec, M.R., 2017. The effects of base-salt relief on salt flow and suprasalt deformation patterns—Part 2: application to the eastern Gulf of Mexico. Interpretation 5 (1), SD25–SD38.
Duval, B., Cramez, C., Jackson, M.P.A., 1992. Raft tectonics in the Kwanza basin, Angola. Mar. Petrol. Geol. 9 (4), 389–404.
Erdi, A., Jackson, C.A.L., 2021. What controls salt-detached contraction in the translational domain of the outer Kwanza Basin, offshore Angola? Basin Res. 33 (3), 1880–1905.
Evans, S.L., Jackson, C.A.L., 2020. Base-salt relief controls salt-related deformation in the Outer Kwanza Basin, offshore Angola. Basin Res. 32 (4), 668–687.
Evans, S.L., Jackson, C.A.L., 2021. Intra-salt structure and strain partitioning in layered evaporites: implications for drilling through Messinian salt in the eastern Mediterranean. Petrol. Geosci. 27 (4).
Evans, S.L., Jackson, C.A.L., Oppo, D., 2021. Taking the pulse of salt-detached gravity gliding in the eastern Mediterranean. Tectonics 40 (7) e2020TC006476.
Ferrer, O., Gratacós, O., Roca, E., Muñoz, J.A., 2017. Modeling the interaction between presalt seamounts and gravitational failure in salt-bearing passive margins: the Messinian case in the northwestern Mediterranean Basin. Interpretation 5 (1), SD99–SD117.
Ferrer, O., Carola, E., McClay, K., Bufaliza, N., 2023. Analogue modeling of domino-style extensional basement fault systems with prekinematic salt. AAPG (Am. Assoc. Pet. Geol.) Bull. 107 (1), 23–47.
Gaullier, V., Brun, J.P., Gue, G., Lecanu, H., 1993. Raft tectonics: the effects of residual topography below a salt decollement. Tectonophysics 228 (3–4), 363–381.
Ge, Z., Rosenau, M., Warsitzka, M., Gawthorpe, R.L., 2019. Overprinting translational domains in passive margin salt basins: insights from analogue modelling. Solid Earth 10 (4), 1283–1300.
Gradmann, S., Beaumont, C., 2017. Numerical modelling study of mechanisms of mid-basin salt canopy evolution and their potential applications to the Northwestern Gulf of Mexico. Basin Res. 29 (4), 490–520.
Hubbert, M.K., 1937. Theory of scale models as applied to the study of geologic structures. Bull. Geol. Soc. Am. 48 (10), 1459–1520.
Hudec, M.R., Jackson, M.P., 2004. Regional restoration across the Kwanza Basin, Angola: salt tectonics triggered by repeated uplift of a metastable passive margin. AAPG Bull. 88 (7), 971–990.
Jackson, M.P., Hudec, M.R., 2005. Stratigraphic record of translation down ramps in a passive-margin salt detachment. J. Struct. Geol. 27 (5), 889–911.
Jackson, M.P.A., Hudec, M.R., 2016. Principles and Practice of Salt Tectonics. Cambridge University Press.
Jackson, M.P., Vendeville, B.C., Schultz-Ela, D.D., 1994. Structural dynamics of salt systems. Annu. Rev. Earth Planet Sci. 22 (1), 93–117.
Jackson, C.A.L., Jackson, M.P., Hudec, M.R., Rodriguez, C.R., 2015. Enigmatic structures within salt walls of the Santos Basin—Part 1: geometry and kinematics from 3D seismic reflection and well data. J. Struct. Geol. 75, 135–162.
Koyi, H., 1997. Analogue modelling: from a qualitative to a quantitative technique—a historical outline. J. Petrol. Geol. 20 (2), 223–238.
Lundin, E.R., 1992. Thin-skinned extensional tectonics on a salt detachment, northern Kwanza Basin, Angola. Mar. Petrol. Geol. 9 (4), 405–411.
Mauduit, T., Gaullier, V., Brun, J.P., Guerin, G., 1997. On the asymmetry of turtle-back growth anticlines. Mar. Petrol. Geol. 14 (7–8), 763–771.
Miró, J., Ferrer, O., Muñoz, J.A., Manastchal, G., 2023. Role of inheritance during tectonic inversion of a rift system in basement-involved to salt-decoupled transition: analogue modelling and application to the Pyrenean–Biscay system. Solid Earth 14 (4), 425–445.
Nettleton, L.L., Elkins, T.A., 1947. Geologic models made from granular materials. Eos, Transactions American Geophysical Union 28 (3), 451–466.
Peel, F.J., 2014. The engines of gravity-driven movement on passive margins: quantifying the relative contribution of spreading vs. gravity sliding mechanisms. Tectonophysics 633, 126–142.
Pichel, L.M., Peel, F., Jackson, C.A., Huuse, M., 2018. Geometry and kinematics of salt-detached ramp syncline basins. J. Struct. Geol. 115, 208–230.
Pichel, L.M., Finch, E., Gawthorpe, R.L., 2019a. The impact of pre-salt rift topography on salt tectonics: a discrete-element modeling approach. Tectonics 38 (4), 1466–1488.
Pichel, L.M., Huuse, M., Redfern, J., Finch, E., 2019b. The influence of base-salt relief, rift topography and regional events on salt tectonics offshore Morocco. Mar. Petrol. Geol. 103, 87–113.
Pichel, L.M., Jackson, C.A.L., Peel, F., Dooley, T.P., 2020. Base-salt relief controls salt-tectonic structural style, São Paulo Plateau, Santos Basin, Brazil. Basin Res. 32 (3), 453–484.
Ramberg, H., 1981. Gravity, Deformation and the Earth's Crust: in Theory, Experiments and Geological Application. Academic press, London, p. 452.
Richard, P., 1991. Experiments on faulting in a two-layer cover sequence overlying a reactivated basement fault with oblique-slip. J. Struct. Geol. 13 (4), 459–469.
Rodriguez, C.R., Jackson, C.A.L., Rotevatn, A., Bell, R.E., Francis, M., 2018. Dual tectonic-climatic controls on salt giant deposition in the Santos Basin, offshore Brazil. Geosphere 14 (1), 215–242.
Roma, M., Ferrer, O., Roca, E., Pla, O., Escosa, F.O., Butillé, M., 2018. Formation and inversion of salt-detached ramp-syncline basins. Results from analog modeling and application to the Columbrets Basin (Western Mediterranean). Tectonophysics 745, 214–228.
Rowan, M.G., Peel, F.J., Vendeville, B.C., 2004. Gravity-driven fold belts on passive margins. Thrust Tectonics and Hydrocarbon Systems, AAPG Memoir 82, 157–182.
Rowan, M.G., Peel, F.J., Vendeville, B.C., Gaullier, V., 2012. Salt tectonics at passive margins: geology versus models–Discussion. Mar. Petrol. Geol. 37 (1), 184–194.
Rowan, M.G., Urai, J.L., Fiduk, J.C., Kukla, P.A., 2019. Deformation of intrasalt competent layers in different modes of salt tectonics. Solid Earth 10 (3), 987–1013.
Rowan, M.G., Tilton, J., Lebit, H., Fiduk, J.C., 2022. Thin-skinned extensional salt tectonics, counterregional faults, and the Albian Gap of Brazil. Mar. Petrol. Geol. 137, 105478.
Schléder, Z., Urai, J.L., 2005. Microstructural evolution of deformation-modified primary halite from the middle triassic röt formation at hengelo, The Netherlands. Int. J. Earth Sci. 94 (5–6), 941–955.
Schléder, Z., Burliga, S., Urai, J.L., 2007. Dynamic and static recrystallization-related microstructures in halite samples from the Kłodawa salt wall (central Poland) as revealed by gamma-irradiation. Neues Jahrbuch Mineral. Abhand.: Journal of Mineralogy and Geochemistry 184 (1), 17–28.
Schultz-Ela, D.D., 2001. Excursus on gravity gliding and gravity spreading. J. Struct. Geol. 23 (5), 725–731.
Spiers, C.J., Urai, J.L., Lister, G.S., 1988. The effect of brine (inherent or added) on rheology and deformation mechanisms in salt rock. In: Second Conference on the Mechanical Behaviour of Salt, Hanover,FRG, September 24-28, 1984. Transtech Publ., Clausthal-Zellerfeld, pp. 89–102.
Spiers, C.J., Carter, N.L., 1998. Microphysics of rocksalt flow in nature. Rock Soil Mech. 115–128.
Stewart, S.A., Ruffell, A.H., Harvey, M.J., 1997. Relationship between basement-linked and gravity-driven fault systems in the UKCS salt basins. Mar. Petrol. Geol. 14 (5), 581–604.
Trusheim, F., 1960. Mechanism of salt migration in northern Germany. AAPG (Am. Assoc. Pet. Geol.) Bull. 44 (9), 1519–1540.
Tucker, M.E., 1991. Sequence stratigraphy of carbonate-evaporite basins: models and application to the Upper Permian (Zechstein) of northeast England and adjoining North Sea. J. Geol. Soc. 148 (6), 1019–1036.
Urai, J.L., Spiers, C.J., Zwart, H.J., Lister, G.S., 1986. Weakening of rock salt by water during long-term creep. Nature 324, 554–557.
Urai, J.L., Schléder, Z., Spiers, C.J., Kukla, P.A., 2008. Flow and transport properties of salt rocks. In: Littke, R., Bayer, U., Gajwski, D., Nelskamp, S. (Eds.), Dynamics of Complex Intracontinental Basins: the Central European Basin System. Springer, Berlin, pp. 277–290.
Vendeville, B., 1988. Modèles expérimentaux de fracturation de la couverture contrôlée par des failles normales dans le socle. Comptes rendus de l'Académie des sciences. Série 2, Mécanique, Physique, Chimie, Sciences de l'univers. Sci. Terre 307 (8), 1013–1018.
Vendeville, B.C., 1989. Scaled experiments on the interaction between salt flow and overburden faulting during syndepositional extension. In: SEPM Gulf Coast Section, 10th Annual Research Conference, Houston, Program and Extended Abstracts, pp. 131–136.
Vendeville, B., Cobbold, P.R., 1988. How normal faulting and sedimentation interact to produce listric fault profiles and stratigraphic wedges. J. Struct. Geol. 10 (7), 649–659.
Vendeville, B., Cobbold, P.R., Davy, P., Brun, J.P., Choukroune, P., 2002. Physical models of extensional tectonics at various scales. Extensional tectonics: faulting and related processes 2, 171–183.
Vendeville, B.C., Jackson, M.P., 1992a. The rise of diapirs during thin-skinned extension. Mar. Petrol. Geol. 9 (4), 331–354.
Vendeville, B.C., Jackson, M.P.A., 1992b. The fall of diapirs during thin-skinned extension. Mar. Petrol. Geol. 9 (4), 354–371.
Warren, J.K., 2016. Evaporites: A Geological Compendium. Springer.

Weijermars, R., Jackson, M.T., Vendeville, B., 1993. Rheological and tectonic modeling of salt provinces. Tectonophysics 217 (1–2), 143–174.
Withjack, M.O., Callaway, S., 2000. Active normal faulting beneath a salt layer: an experimental study of deformation patterns in the cover sequence. AAPG Bull. 84 (5), 627–651.
Zwaan, F., Schreurs, G., 2017. How oblique extension and structural inheritance influence rift segment interaction: insights from 4D analog models. Interpretation 5 (1), SD119–SD138.